PNAS
www.pnas.org

Supplementary Information for

PD-1^{+} regulatory T cells amplified by PD-1 blockade promote hyperprogression of cancer

Takahiro Kamada, Yosuke Togashi, Christopher Tay, Danbee Ha, Akinori Sasaki, Yoshiaki Nakamura, Eiichi Sato, Shota Fukuoka, Yasuko Tada, Atsushi Tanaka, Hiromasa Morikawa, Akihito Kawazoe, Takahiro Kinoshita, Kohei Shitara, Shimon Sakaguchi and Hiroyoshi Nishikawa

Hiroyoshi Nishikawa, M.D., Ph.D.
E-mail: hnishika@ncc.go.jp

Shimon Sakaguchi, M.D., Ph.D.
E-mail: shimon@ifrec.osaka-u.ac.jp

This PDF file includes:

Supplementary text
Figs. S1 to S8
Tables S1 to S7
References for SI reference citations

Supplementary Information Text

Materials and Methods:

Patients and samples

Patients with advanced GC who received anti-PD-1 mAb (nivolumab) from October to December 2017 and underwent at least one image evaluation for clinical responses until 2 months after the initial drug administration at National Cancer Center Hospital East were enrolled in this study (**Table S1**). FFPE slides from pre-treatment biopsy specimens were used for genome analyses, and fresh paired tumor samples obtained from primary or metastatic tumor by endoscopic or needle biopsy at pre- and post-nivolumab (just before the initial drug administration and at first evaluation, respectively) were subjected to immunological assays. Patients with Eastern Clinical Oncology Group PS 2 or higher were excluded from this study. In addition, 22 patients with GC who underwent surgical resection at National Cancer Center Hospital East from September to December 2015 were also enrolled for TIL analyses (**Table S5**).

Definition of HPD

Tumor size was evaluated as the sum of the longest diameters of the target lesions following the Response Evaluation Criteria in Solid Tumors (RECIST 1.1) criteria (1). HPD was defined as previously reported; time-to-treatment failure <2 months, >50% increase in tumor burden compared with pre-treatment imaging, and >2-fold increase in progression speed (2).

Immunohistochemistry

Anti-PD-L1 mAb (SP263, Ventana, Tucson, AZ) was used for IHC using an automatic staining instrument (BenchMark ULTRA, Ventana). PD-L1 positivity was defined as staining in 1% or more in tumor or stroma cells. Multiplexed fluorescent immunohistochemistry was performed by the TSA method using an Opal IHC kit (PerkinElmer, Waltham, MA) according to the manufacturer's instructions. Anti-human CD4 mAb [clone 4B12, DAKO, Glostrup, Denmark, working concentration (WC) 10 μg/ml], anti-human FoxP3 mAb (clone 236A/E7, Abcam, Cambridge, UK, WC 8 μg/ml) were used as primary antibodies. Multiplexed fluorescent labeled images of three

randomly selected fields (669x500 micrometer) were captured with an automated imaging system (Vectra ver3.0, PerkinElmer). Cell counts were performed manually on each image.

Evaluation of mismatch repair (MMR) status

MMR status was examined with IHC with anti-mutLhomolog 1 (MLH1; ES05) mAb, anti-mutS homolog 2 (MSH2; FE11) mAb, anti-postmeiotic segregation increased 2 (PMS2; EP51) mAb, and anti-mutShomolog 6 (MSH6; EP49) mAb (Dako, Copenhagen, Denmark). Tumors were considered negative for MLH1, MSH2, PMS2, or MSH6 expression only if there was a complete absence of nuclear staining in the tumor cells, and normal epithelial cells and lymphocytes were used as an internal control. Tumors lacking MLH1, MSH2, PMS2, or MSH6 expression were defined as MMR deficient, whereas tumors that maintained expression of all markers were considered MMR proficient.

Evaluation of Epstein-Barr virus (EBV) infection

Chromogenic *in situ* hybridization (ISH) for EBV-encoded RNA was performed with fluorescein-labeled oligonucleotide probes (INFORM EBER probe) with enzymatic digestion (ISH protease 3, Ventana) and an iViewBlue detection kit (Ventana) with use of the BenchMark ULTRA staining system.

Genomic analysis

DNA and RNA were extracted from FFPE tumor samples and were subjected to the Oncomine™ Comprehensive Assay version 3 (Thermo Fisher Scientific) which allows to detect gene mutations, copy number variants and fusions across multiple genes (**Table S3**). The detected genomic variant data were classified according to genetic drivers of cancer including gain- and loss-of-function mutations or single nucleotide variants based on the Oncomine Knowledgebase.

PBMC and TIL analysis

PBMCs were isolated by density gradient centrifugation with Ficoll-Paque (GE Healthcare, Little Chalfont, UK). To collect TILs, tumor tissues were minced and treated with gentleMACS Dissociator (Miltenyi Biotec), as previously described (3) and the prepared cells (TILs) were subjected to flow cytometric analysis.

Animal procedures

C57BL/6J mice were purchased from CLEA, Japan (Tokyo, Japan). CD45.1 C57BL/6J mice were maintained in Osaka University animal facility. Mice on $CD4^{Cre}$ (4) and $FoxP3^{IRES\text{-}Cre}$ (5) and $FoxP3^{IRES\text{-}DTR\text{-}GFP}$ (FDG) (6) mice were described previously. $PD1^{Floxed}$ mice were generated by first cloning the targeting construct and transfecting into TT2 (C57BL/6N x CBA) ES cells (Accession No. CDB1074K: Animal Resource Development Unit and Genetic Engineering Team, Riken Center for Life Science Technologies). Mice were then crossed to FLPe to delete frt flanked neomycin resistance gene and backcrossed to C57BL/6J background 10 times before further crossing with C57BL/6J $CD4^{Cre}$FDG and $FoxP3^{IRES\text{-}Cre}$ mice (**Fig. S4**).

For adoptive cell transfer experiments, $CD44^{-}CD62L^{+}CD4^{+}CD25^{+}$ Treg cells were isolated from $FoxP3^{IRES\text{-}Cre}$, $FoxP3^{IRES\text{-}Cre}PD1^{Floxed}$ and CD45.1 mice by first enriching for $CD4^{+}$ cells using CD4 Isolation kit (Miltenyi Biotec, Bergisch Gladbach, Germany) then surface stained and sorted on FACS AriaSorp (BD Biosciences, Franklin Lakes, NJ, USA). Cells were expanded in culture with CD3/CD28 dynabeads (Thermo Fisher Scientific, Waltham, MA) according to manufacturer's instructions for 7 days in RPMI 1640 supplemented with 10% fetal calf serum (FCS), penicillin–streptomycin, 2-mercaptoethanol, 10mM HEPES and 1mM sodium pyruvate. Spleen cells were collected from $CD4^{Cre}PD1^{Floxed}$FDG mice and mixed with either $FoxP3^{IRES\text{-}Cre}$ or $FoxP3^{IRES\text{-}Cre}PD1^{Floxed}$ Treg cells for transfer into C57BL/6J mice that were irradiated (6 Gy) 24 hours before cell transfer. Each mouse received $3x10^{7}$ $CD4^{Cre}PD1^{Floxed}$FDG spleen cells and $3x10^{5}$ Treg cells. Following cell transfer, mice were inoculated with $1x10^{5}$ B16F0 cells subcutaneously. Diphtheria toxin (DT) was administered (1 μg/mouse) intraperitoneally on day 3 after cell transfer. At indicated times, anti-PD-1 (clone 29F.1A12; Bio X cell, New Haven, CT) or isotype-matched IgG (clone 2A3; Bio X cell) mAb (200 μg/mouse) were intravenously administered.

BMC mice were generated by first irradiating CD45.1 mice with 2x5 Gy with a 4-hour interval between doses. BM cells collected from the femur and tibia of non-irradiated donor mice were T cell-depleted and mixed to obtain an inoculum comprising 70% CD45.1 and 30% CD45.2 $CD4^{Cre}PD1^{floxed}$FDG which was then transferred into recipient mice intravenously. BMC mice were assessed 6 weeks post-transplantation.

All mice were maintained in specific pathogen free facility in Osaka University. All experiments were approved by the Institutional Review Board and performed according to guidelines for animal welfare set by Osaka University.

Flow cytometry for human samples

Cells, washed by PBS with 2% fetal calf serum, were stained with mAbs specific for CD3, CD4, CD8, CD45RA, CCR7, CD28, PD-1, CTLA-4, LAG-3, OX-40, CCR4, and with Live/Dead cell viability dye (Thermo Fisher Scientific). After staining of cell surface markers, cells were intracellularly stained for FoxP3 and Ki67 with FoxP3 Staining Buffer Set (eBioscience, Santa Clara, CA) according to the manufacturer's instructions. After washing, cells were analyzed with BD LSRFortessa^{TM} X-20 (BD Biosciences) and FlowJo software (Treestar, Ashland, OR). Staining antibodies were diluted according to the manufacturer's instructions. The detailed information of antibodies used are summarized in **Table S6**.

Flow cytometry for mouse samples

Single cell suspensions were prepared from tumors, spleen and lymph nodes. Cells were first incubated with anti-CD16/32 then stained with Live/Dead cell viability dye, and antibodies for surface markers as follows. B220, CD45.1, CD45.2, CD11c, CD4, CD8, CD44, CD62L, and PD-1. Cells were subsequently fixed and permeabilized with Foxp3/Transcription staining buffer set (BD Biosciences) followed by staining for intracellular Ki67 and FoxP3. Stained cells were detected using BD LSR Fortessa^{TM} and analyzed using FlowJo software. T cells were analyzed after gating for live $B220^{-}CD11c^{-}$ cells. The detailed information of antibodies used are summarized in **Table S7**.

Suppression assay for human cells

PD-1^{+}CD45RA^{-}CD25^{high}CD4^{+} T cells (eTreg cells) were sorted from PBMCs of healthy individuals using FACS Aria Fusion (BD Biosciences). 1x10^{4} CFSE-labeled (1 μM) responder CD8^{+} T cells from PBMCs were co-cultured with/without unlabeled PD-1^{+} eTreg cells in the presence of 1x10^{5} irradiated APCs and 0.5 μg/ml anti-CD3 (OKT3) mAb. For PD-1 blockade, anti-PD-1 mAb (nivolumab) kindly provided by Ono Pharmaceutical Co Ltd) or control isotype-matched mAb was added. Cell proliferation was assessed 5 days later by dilution of CFSE-labeled cells with flow cytometry.

Suppression assay for mouse cells

Splenic CD4^{+} T cells and CD11c^{+} dendritic cells were first enriched using CD4 T cell isolation kit and CD11c microbeads (Miltenyi Biotec), respectively, according to manufacturer's instructions. After enrichment, cells were stained and sorted for CD4^{+}FoxP3^{GFP-} Tconv cells, CD4^{+}FoxP3^{GFP+} Treg cells and CD11c^{+} dendritic cells. Sorted Tconv cells were stained with CellTrace violet (CTV) (Thermo Fisher Scientific). 1.5x10^{4} Tconv cells were cultured with Treg cells at indicated Treg:Tconv ratios with 7.5x10^{3} dendritic cells in the presence of anti-CD3 mAb (0.5 μg/ml). For PD-1 blockade, either anti-PD-1 or isotype-matched mAb (15 μg/ml) was added. Cell proliferation was assessed 3 days later by dilution of CTV-labeled Tconv cells with flow cytometry.

Cellular proliferation

PD-1^{-} or PD-1^{+} eTreg cells were sorted from PBMCs of heathy individuals and were cultured with/without PD-L1 Fc immunoglobulin (R & D systems, Minneapolis, MN) and/or anti-PD-1 mAb in the presence of anti-CD3 mAb and anti-CD28 mAb (Thermo Fisher Scientific). Forty-eight hours after incubation, cellular proliferation was evaluated using WST-1 assay (TaKaRa, Shiga, Japan).

Statistical analysis

The patient characteristics were compared between HPD and non-HPD using the Fisher exact test. Continuous variables were analyzed using t-test. The statistical analyses were two-tailed and were performed using Prism version 7 software (GraphPad Software, Inc.,

La Jolla, CA). A *P*-value of less than 0.05 was considered statistically significant. For mouse experiments, comparisons between two experimental groups were carried out using non-parametric Mann-Whitney U test. Two-way ANOVA and Sidak's multiple comparisons test were applied in grouped analyses for *in vitro* suppression assay and tumor growth kinetics. Data are presented as mean ± SEM and analyzed using GraphPad Prism as above. $P<0.05$ was considered statistically significant.

Fig. S1. Genomic features of patients who experienced HPD during PD-1 blockade treatment.

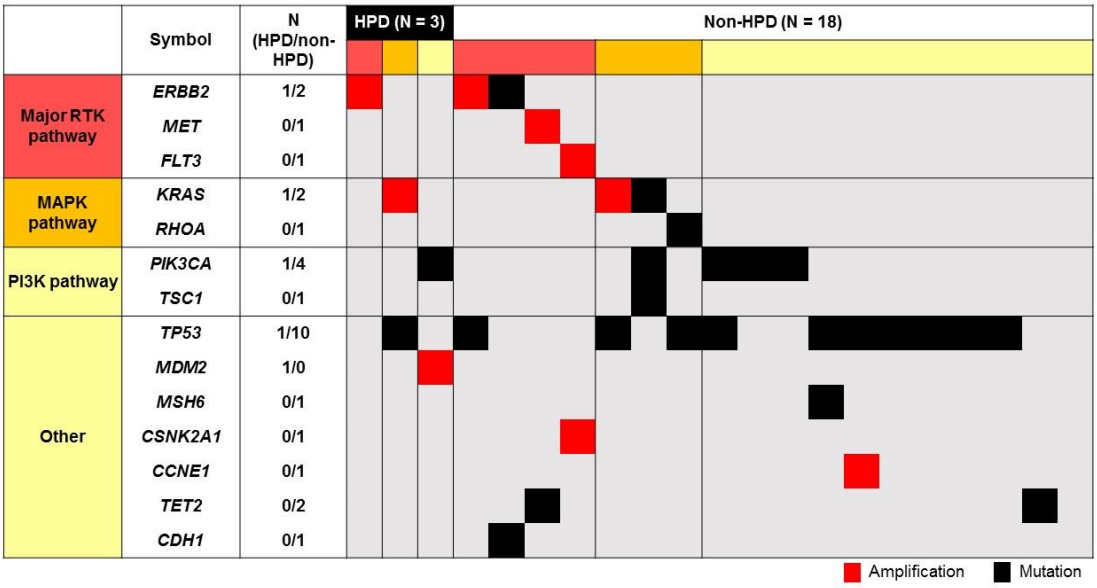

DNA and RNA extracted from FFPE tumor samples (3 HPD patients and 18 non-HPD patients) were subjected to the Oncomine™ Comprehensive Assay version 3, that can detect gene mutations, copy number variants and fusions across multiple genes (**Table S3**). Gene alterations are shown in red (amplification) and black (mutation). One among three patients with HPD possessed an MDM2 gene amplification, whereas no patients without HPD had MDM2 gene family alterations. Other gene alterations found in patients with HPD (*ERBB2* amplification, *KRAS* amplification, *TP53* mutation, and *PIK3CA* mutation) were also detected in non-HPD patients.

Fig. S2. Kinetic changes of eTreg cells, PD-1$^+$ eTreg cells, CTLA-4$^+$ eTreg cells, and Ki67$^+$ eTreg cells in PBMCs during anti-PD-1 mAb treatment.

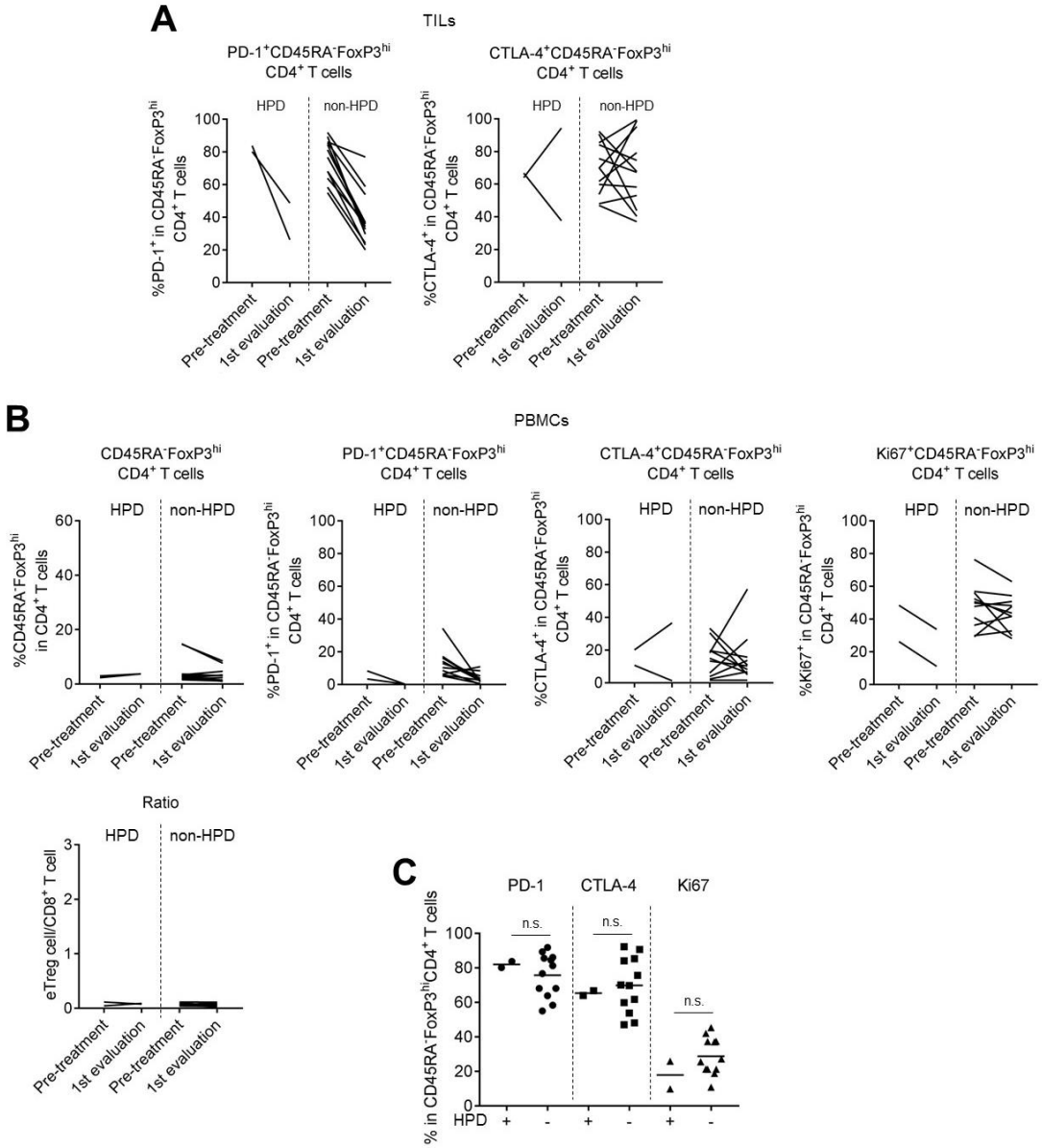

TILs and PBMCs collected from 14 GC patients before and after anti-PD-1 mAb treatment were subjected to flow cytometry as in **Fig. 2**. Summary of kinetic changes of eTreg cells, PD-1$^+$ eTreg cells, CTLA-4$^+$ eTreg cells and Ki-67$^+$ eTreg cells in TILs (**A**) and PBMCs (**B**) from pre-treatment to 1st evaluation. PD-1, CTLA-4, and Ki67 expressions by eTreg cells in TILs before anti-PD-1 mAb treatment are also summarized (**C**).

Fig. S3. Kinetic changes of Ki67$^+$CD8$^+$ cells in TILs during anti-PD-1 mAb treatment.

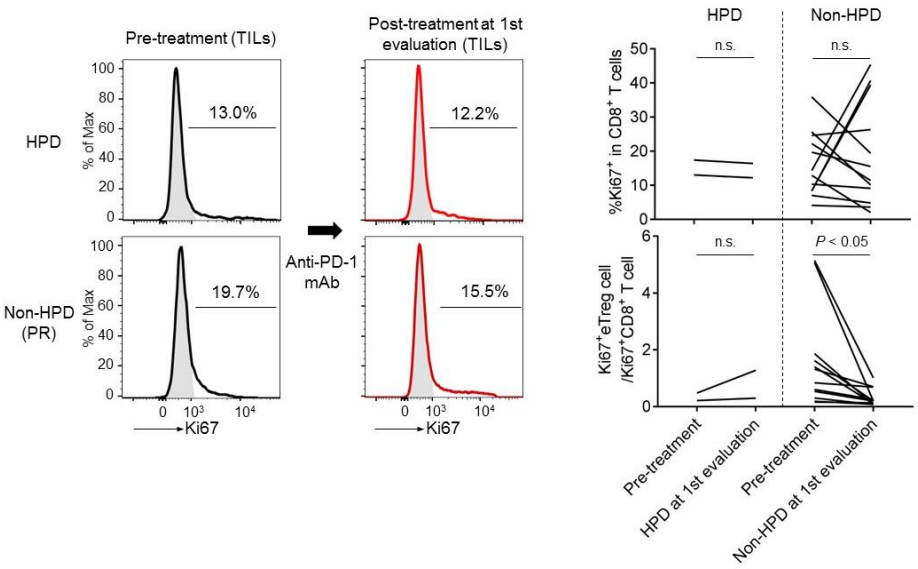

TILs collected from 14 GC patients before and after anti-PD-1 mAb treatment were subjected to flow cytometry as in **Fig. 2**. **Left,** Representative staining of Ki67 by CD8$^+$ T cells in TILs of kinetic changes from pre-treatment to 1st evaluation. Black, anti-PD-1 mAb (-); Red, anti-PD-1 mAb (+); Gray, isotype control. **Right,** Summaries of kinetic changes of Ki67$^+$CD8$^+$ T cells and the ratio of Ki67$^+$ eTreg cells/ Ki67$^+$CD8$^+$ T cells in two HPD patients and 12 non-HPD patients. n.s., not significant.

Fig. S4. PD-1 expression by eTreg cells used for suppression and cellular proliferation assays.

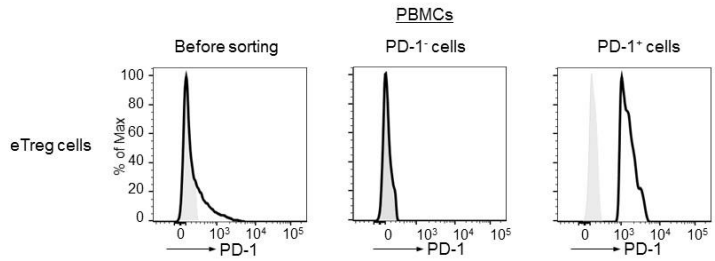

PD-1^{+} eTreg cells were sorted from PBMCs using FACS Aria fusion and PD-1 expression was confirmed before using suppression and cellular proliferation assays.

Fig. S5. Targeting of mouse PD-1 gene.

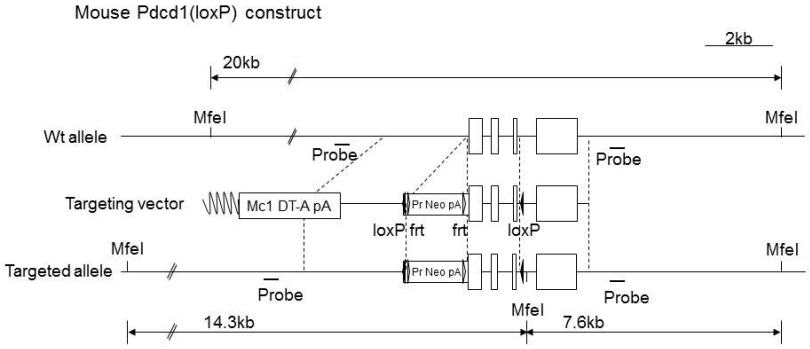

Schematic map of the targeting construct for mouse PD-1^{floxed} locus is shown.

Fig. S6. Effect of depleting PD-1-deficient Treg cells on tumor development.

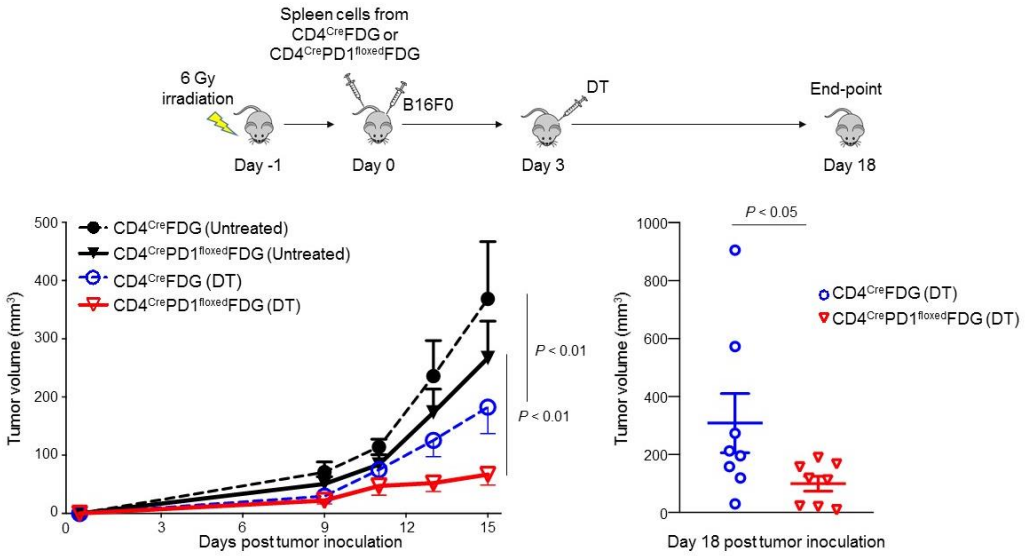

C57BL/6J mice were 6 Gy irradiated for lymphodepletion. Mice were then transferred with spleen cells from either CD4^{Cre}FDG or CD4^{Cre}PD1^{floxed}FDG mice and inoculated with B16F0 cells. On day 3, mice in each group were either administered with diphtheria toxin (DT) to deplete transferred Treg cells or left untreated. **Left,** Growth of B16 tumor measured over 15 days. n=8/group. **Right,** Summary of tumor volume for CD4^{Cre}FDG (DT) and CD4^{Cre}PD1^{floxed}FDG (DT) groups measured on day 18 post-inoculation.

Fig. S7. Therapeutic targets of eTreg cells, which can be activated by PD-1 blockade, subsequently contribute to HPD.

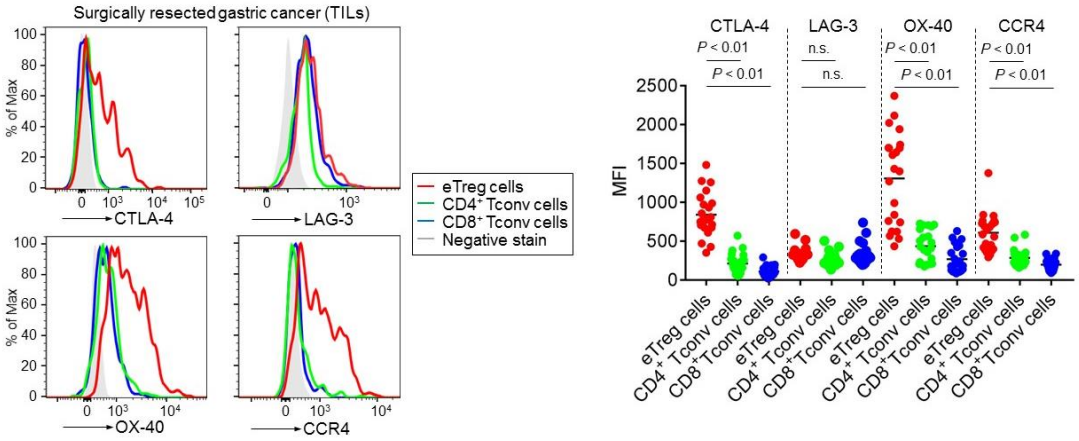

TILs were collected from surgically resected GC samples (**Table S5**) and were subjected to flow cytometry. **Left,** Representative flow cytometry plots for CTLA-4, LAG-3, OX-40 and CCR4 by eTreg cells, FoxP3$^-$CD4$^+$ Tconv cells, and CD8$^+$ Tconv cells in TILs. Red, eTreg cells; green, FoxP3$^-$CD4$^+$ Tconv cells; blue, CD8$^+$ Tconv cells; gray, negative stain. **Right,** Summary of CTLA-4, LAG-3, OX-40 and CCR4 expression by eTreg cells, FoxP3$^-$CD4$^+$ Tconv cells, and CD8$^+$ Tconv cells in 22 GC patients. n.s., not significant.

Fig. S8. A graphical summary schema of the role of PD-1 in Treg-cell-mediated immune suppressive function.

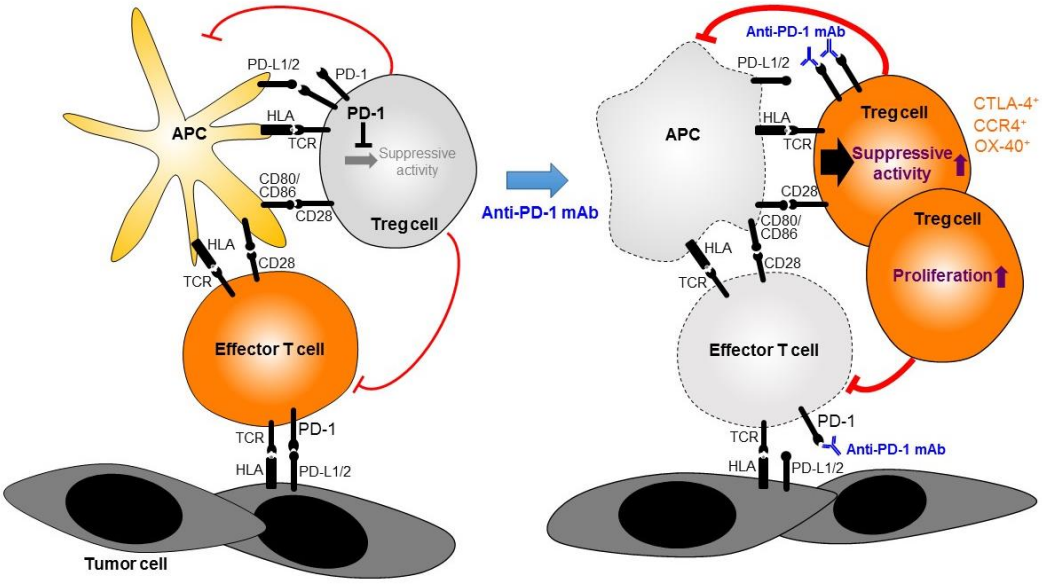

PD-1 expression inhibits TCR and CD28 signals in Treg cells and thereby attenuates Treg-cell-mediated immune suppression (**Left**). PD-1 blockade by anti-PD-1 antibody increases TCR and CD28 signal in Treg cells, and thereby enhances their proliferation and suppressive activity. Strong immune suppression by such expanded and activated eTreg cells hampers activation of effector T cells such as $CD8^+$ T cells (**Right**).

Table S1. Clinicopathological features of patients who experienced HPD after PD-1 blockade.

Features	Non-HPD (n=32)	HPD (n=4)	*P* value
Age [Median] (range)	64.5 (41-86)	72 (56-82)	0.316
Sex Male/female	27/5	3/1	0.535
Histology Intestinal/diffuse/mix	13/17/2	2/2/0	1.000¶
HER2 Positive/negative	6/26	2/2	0.207
MMR Proficient/deficient/unknown	24/5/3	4/0/0	1.000
EBV Positive/negative/unknown	2/27/3	0/4/0	1.000
PD-L1 Positive/negative/unknown	25/4/3	3/1/0	0.500
Stage IV/recurrence after surgery	17/15	4/0	0.123
Number of metastatic organs [median] (range)	2 (1-4)	3 (2-4)	0.140
Liver metastasis Positive/negative	17/15	3/1	0.613
Treatment line 3nd line/4rd line-	20/12	3/1	1.000
Response at 1st tumor evaluation PR/SD/PD	9/10/13	0/0/4	

¶Intestinal vs. diffuse.

Table S2. Summary of patients who experienced HPD after PD-1 blockade.

Case	Sex	Age	Histology	PD-L1	EBV	MMR	HER2	Genomic features	Immunological features	PFS after PD-1 blockade (day)	OS after PD-1 blockade (day, status)
1	Female	71	Intestinal	Positive	Negative	Proficient	Positive	*ERBB2* amplification	$Ki67^+$eTreg cell, 40.2%	62	>62, alive
2	Male	56	Diffuse	Positive	Negative	Proficient	Negative	*TP53 p.Arg282Trp* *KRAS* amplification	NA	15	20, dead
3	Male	73	Intestinal	Positive	Negative	Proficient	Negative	*PIK3CA p.Cys420Arg* *MDM2* amplification	$Ki67^+$eTreg cell, 21.1%	36	55, dead
4	Male	82	Diffuse	Negative	Negative	Proficient	Positive	NA	NA	20	65, dead

MMR, mismatch repair; eTreg cell, effector regulatory T cell; PFS, progression-free survival; OS, overall survival; NA, not assessed.

Table S3. Gene list of the Oncomine™ Comprehensive Assay version 3

Hotspot genes	Full-length genes	Copy number genes	Gene fusions (inter- and intragenic)
AKT1	*ATM*	*AKT1*	*ALK*
ALK	*BAP1*	*AR*	*AXL*
AR	*BRCA1*	*CCND1*	*BRAF*
ARAF	*BRCA2*	*CCNE1*	*EGFR*
BRAF	*CDKN2A*	*CDK4*	*ERBB2*
BTK	*FBXW7*	*CDK6*	*ERG*
CBL	*MSH2*	*EGFR*	*ETV1*
CDK4	*NF1*	*ERBB2*	*ETV4*
CHEK2	*NF2*	*FGFR1*	*ETV5*
CSF1R	*NOTCH1*	*FGFR2*	*FGFR1*
CTNNB1	*PIK3R1*	*FGFR3*	*FGFR2*
DDR2	*PTCH1*	*FGFR4*	*FGFR3*
EGFR	*PTEN*	*FLT3*	*NTRK1*
ERBB2	*RB1*	*IGF1R*	*NTRK3*
ERB83	*SMARCB1*	*KIT*	*PDGFRA*
ERBB4	*STK11*	*KRAS*	*PPARG*
ESR1	*TP53*	*MDM2*	*RAF1*
EZH2	*TSC1*	*MDM4*	*RET*
FGFR1	*TSC2*	*MET*	*ROS1*
FGFR2	*ARID1A*	*MYC*	*AKT2*
FGFR3	*ATR*	*MYCL*	*AR*
FLT3	*ATRX*	*MYCN*	*BRCA1*
FOXL2	*CDK12*	*PDGFRA*	*BRCA2*
GATA2	*CDKN1B*	*PIK3CA*	*CDKN2A*
GNA11	*CDKN2B*	*PPARG*	*ERB84*
GNAQ	*CHEK1*	*TERT*	*ESR1*
GNAS	*CREBBP*	*AKT2*	*FGR*
HNF1A	*FANCA*	*AKT3*	*FLT3*
HRAS	*FANCD2*	*ALK*	*JAK2*
IDH1	*FANCI*	*AXL*	*KRAS*
IDH2	*MLH1*	*BRAF*	*MDM4*
JAK1	*MRE11A*	*CCND2*	*MET*
JAK2	*MSH6*	*CCND3*	*MYB*
JAK3	*NBN*	*CDK2*	*MYBL1*
KDR	*NOTCH2*	*CDKN2A*	*NF1*
KIT	*NOTCH3*	*CDKN2B*	*NOTCH1*
KNSTRN	*PALB2*	*ESR1*	*NOTCH4*
KRAS	*PMS2*	*FGF19*	*NRG1*
MAGOH	*POLE*	*FGF3*	*NTRK2*
MAP2K1	*RAD50*	*NTRK1*	*NUTM1*

MAP2K2	*RAD51*	*NTRK2*	*PDGFRB*
MAPK1	*RAD51B*	*NTRK3*	*PIK3CA*
MAX	*RAD51C*	*PDGFRB*	*PRKACA*
MED12	*RAD51D*	*PIK3CB*	*PRKACB*
MET	*RNF43*	*RICTOR*	*PTEN*
MTOR	*SETD2*	*TSC1*	*RAD51B*
MYD88	*SLX4*	*TSC2*	*RB1*
NFE2L2	*SMARCA4*		*RELA*
NRAS			*RSPO2*
PDGFRA			*RSPO3*
PIK3CA			*TERT*
PPP2R1A			
PTPN11			
RAC1			
RAF1			
RET			
RHEB			
RHOA			
SF3B1			
SMO			
SPOP			
SRC			
STAT3			
U2AF1			
XPO1			
AKT2			
AKT3			
AXL			
CCND1			
CDK6			
ERCC2			
FGFR4			
H3F3A			
HIST1H3B			
MAP2K4			
MDM4			
MYC			
MYCN			
NTRK1			
NTRK2			
PDGFRB			
PIK3CB			
ROS1			
SMAD4			
TERT			

TOP1			

Table S4. Gene alterations in all patients

Non-HPD or HPD	Gene mutation	Gene amplification	Fusion
HPD	None	*ERBB2*	None
HPD	*TP53 p.Arg282Trp*	*KRAS*	None
HPD	*PIK3CA p.Cys420Arg*	*MDM2*	None
Non-HPD	None	None	None
Non-HPD	*TP53 p.Gly245Ser*	None	None
Non-HPD	*CDH1 p.Asp254Tyr, ERBB2 p.Arg678Gln*	None	None
Non-HPD	None	*CSNK2A1, FLT3, ZNF217*	None
Non-HPD	*MET p.Asn375Lys, TET2 p.Phe868Leu*	None	None
Non-HPD	*TP53 p.Arg175His*	None	None
Non-HPD	*PIK3CA p.Gly106Val, PIK3CA p.Ala1066Val, TP53 p.Ser240Gly, TP53 p.Pro191del*	None	None
Non-HPD	*TSC1 p.Arg786Ter, PIK3CA p.Tyr1021Cys, PIK3CA p.Gly118Asp, KRAS p.Gly12Asp*	None	None
Non-HPD	*PIK3CA p.Gln546Lys*	None	None
Non-HPD	*TP53 p.Arg273His*	None	None
Non-HPD	*TP53 p.Arg273Cys, RHOA p.Tyr42Cys*	None	None
Non-HPD	*TP53 p.Ala159Val*	None	None
Non-HPD	*TP53 p.Arg175His*	*ERBB2*	None
Non-HPD	*TP53 p.Gly245Ser*	*CCNE1*	None
Non-HPD	*TET2 p.Arg1452Ter*	None	None
Non-HPD	*PIK3CA p.Glu542Lys*	None	None
Non-HPD	*MSH6 p.Lys1358fs, TP53 p.Tyr163Ser*	None	None
Non-HPD	*TP53 p.Arg213Ter*	*KRAS*	None

Table S5. Patient characteristics of surgically resected GC samples

Features	**N = 22**
Age [Median] (range)	71.5 (54-86)
Sex	
Male	14
Female	8
Histology	
Intestinal	15
Diffuse	7
Pathological stage	
I	4
II	10
III	6
IV	2

Table S6. Antibodies used for multicolor flow-cytometry in humans

Antibody	Clone	Company	Conjugation
CD3	UCHT1	BD Biosciences	AF-700
CD4	RPA-T4	BD Biosciences	V500
CD8	RPA-T8	BioLegend	BV785
CD45RA	HI100	BioLegend	BV711
CCR7	G043H7	BioLegend	BV605
PD-1	MIH4*	BD Biosciences	BV421
CTLA-4	L3D10	BioLegend	APC
LAG-3	17B4	Enzo	FITC
OX-40	ACT35	BD Biosciences	PerCP-Cy5.5
CCR4	1G1	BD Biosciences	PE-Cy7
FoxP3	236A/E7	eBioscience	PE
Ki67	20Raj1	eBioscience	PerCP-eFluor710
CD28	CD28.2	BioLegend	BV421

*Anti-PD-1 mAb (MIH4) used for flow cytometry binds to an epitope that is distinct from the epitope bound by nivolumab.

Table S7. Antibodies used for multicolor flow-cytometry in mice

Antibody	Clone	Company	Conjugation
B220	RA3-6B2	eBioscience	APC eFluor780
CD11c	N418	eBioscience	APC eFluor780
CD45.1	A20	eBioscience	eFluor450
CD45.2	104	BD Biosciences	V450
CD4	RM4-5	BioLegend	BV711
CD8	53-6.7	eBioscience	APC
CD62L	MEL14	BioLegend	BV510
CD44	IM7	eBioscience	PE
PD-1	RMP1-30	BioLegend	PE-Cy7
FoxP3	FJK-16s	eBioscience	FITC or PE-Cy7
Ki67	SolA15	eBioscience	PE-Cy7 or eFluor450

References

1. Eisenhauer EA*, et al.* (2009) New response evaluation criteria in solid tumours: revised RECIST guideline (version 1.1). *Eur J Cancer* 45(2):228-247.
2. Champiat S*, et al.* (2017) Hyperprogressive Disease Is a New Pattern of Progression in Cancer Patients Treated by Anti-PD-1/PD-L1. *Clin Cancer Res* 23(8):1920-1928.
3. Saito T*, et al.* (2016) Two $FOXP3^{+}CD4^{+}$ T cell subpopulations distinctly control the prognosis of colorectal cancers. *Nat Med* 22(6):679-684.
4. Lee PP*, et al.* (2001) A critical role for Dnmt1 and DNA methylation in T cell development, function, and survival. *Immunity* 15(5):763-774.
5. Wing K*, et al.* (2008) CTLA-4 control over $Foxp3^{+}$ regulatory T cell function. *Science* 322(5899):271-275.
6. Kim JM, Rasmussen JP, & Rudensky AY (2007) Regulatory T cells prevent catastrophic autoimmunity throughout the lifespan of mice. *Nat Immunol* 8(2):191-197.